

PROTON STRUCTURE AND THE LAMB SHIFT IN HYDROGEN-LIKE ATOMS¹

ÉVA GAJZÁGÓ*, Budapest

The present state of the Lamb shift in hydrogen and muonic is briefly reviewed. Attention is paid particularly to the contributions due to the polarizability of the proton and to the structure of the proton as revealed by the recent experiments concerning the deep inelastic electron-proton scattering.

1. INTRODUCTION

Historically it was the measurement of the $2S_{1/2}$ and $2P_{1/2}$ level displacement in the hydrogen atom which led to the development of quantum electrodynamics. More recently this testing ground has been extended to other hydrogenic atoms including positronium (e^+e^-) muonium (μ^+e^-), and muonic hydrogen (μ^-p). We are interested here in the influence of the proton structure on the spectra of the ordinary and muonic hydrogen, while the other two are important tests of pure electrodynamical systems.

First, I would like to summarize briefly our present knowledge of the spectra of ordinary and muonic hydrogen. In quantum electrodynamics these systems can be treated within the Bethe-Salpeter equation (BSE), which has the form for the hydrogen atom [1]:

$$(\mu_m \hat{P} + \hat{p} - m)(\hat{p} - \mu_M \hat{P} + M) \Psi(p) = \int \frac{d^4 p'}{(2\pi)^4} I(p, p'; P) \Psi(p'), \quad (1)$$

where P is the four momentum of the center-of-mass, p and p' are the relative four momenta of the two particles in the initial and final states ($\mu_m = m_e/(m_e + M_p)$, $\mu_M = M_p/(m_e + M_p)$). $\Psi(p)$ is the wave function of the rela-

¹ Talk given at Elementary Particle Physics Seminar at Pezinská Baba, October 16-18, 1972.

* Atomfizikai Tanszék, Eötvös Loránd Egyetem, BUDAPEST VIII, Puskin u. 5-7, Hungary.

tivistic bound state (the motion of the center-of-mass has been separated), and $I(p, p'; P)$ denotes the sum of all the irreducible graphs.

The dominant interaction of the atom, the Coulomb potential $V = -\alpha/r$ can be separated from the rest of the electromagnetic interaction most readily if we use the radiation gauge in the atomic center-of-mass system. The Coulomb interaction, which must be treated to all orders in the perturbation theory, can then be separated from the Feynman propagator for the exchanged photons. The remainder describes the transverse interaction:

$$D_{\mu\nu}^T = \frac{-g_{\mu\nu} - \delta_{\mu 0} \delta_{\nu 0}}{q^2 + i\epsilon} \frac{\delta_{\mu 0} \delta_{\nu 0}}{|q|^2}. \quad (2)$$

Now, we can consider the BSE with the Coulomb kernel as the unperturbed one, and the remainder irreducible kernels as small perturbations. Within the BSE we get the corrections of the energy levels for the relativistic bound system due to a small perturbation ΔI with the aid of the formula [1]:

$$\Delta E_n = -\frac{i\pi}{2m_e M_p} \int \frac{d^4 p}{(2\pi)^4} \int \frac{d^4 p'}{(2\pi)^4} \bar{\Psi}_n(p) \Delta I(p, p'; P) \Psi_n(p'). \quad (3)$$

The typical irreducible kernels which must be considered for the hydrogen atom, and the corresponding order of magnitude of the corrections are given in Fig. 1.

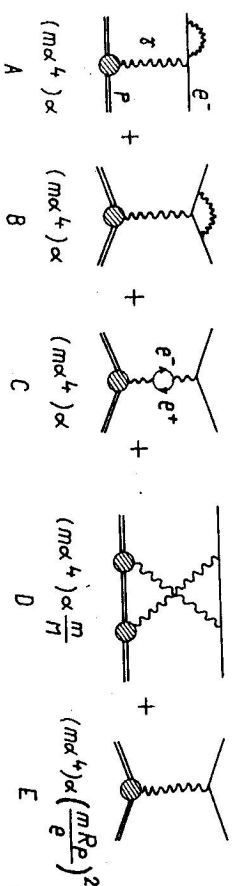


Fig. 1. A — self energy; B — anomalous magnetic moment; C — vacuum polarization; D — recoil correction; E — finite size correction.

Thus we can see that modifications occur from the self energy correction to the bound electron, the anomalous magnetic moment of the electron, the vacuum polarization effects — these are the main contributions — and smaller corrections arise from the recoil effects, finite proton size and other higher order diagrams. The various contributing terms can be classified in terms of the small parameters of the theory: α , m_e/M_p , $\alpha m_e R_p = R_p/a_0$ (where R_p is the nuclear radius).

The comparison of theory with experiment now shows a quite satisfactory agreement:

$$\begin{aligned} \text{Theory: } & 1057.91 \pm 0.16 \text{ MHz} \\ \text{Experiment—theory: } & -0.01 \text{ MHz.} \end{aligned}$$

What can we say now about muonic hydrogen? If there were no electrons, the treatment of the (μ^-p) system would be exactly the same as that of ordinary hydrogen: one has only to replace the mass of the electron with that of the muon in all formulae. However, for the so-called "mixed diagrams" — diagrams containing muons and electrons — the situation is not so simple. It can be shown [2], that the relevant effect of electrons is a contribution to vacuum polarization producing a modification of the photon propagator in a range of the order of the electron Compton wave length $\lambda_e = \hbar/m_e c$. Since λ_e is just of the order of the Bohr-radius of the muon in muonic hydrogen ($\sim \hbar/c m_\mu c$), the μ^-p system will be very sensitive for this effect. Indeed, it has been shown [2] that main contribution to the Lamb shift in muonic hydrogen comes from electron vacuum polarization effects (Fig. 2), while

$$-1.4977 \pm 0.0006 \alpha^2 R_y \quad + \quad \left\{ \begin{array}{l} \text{Diagram 1} \\ \text{Diagram 2} \\ \text{Diagram 3} \\ \text{Diagram 4} \\ \text{Diagram 5} \\ \text{Diagram 6} \\ \text{Diagram 7} \\ \text{Diagram 8} \\ \text{Diagram 9} \\ \text{Diagram 10} \\ \text{Diagram 11} \\ \text{Diagram 12} \\ \text{Diagram 13} \\ \text{Diagram 14} \\ \text{Diagram 15} \\ \text{Diagram 16} \\ \text{Diagram 17} \\ \text{Diagram 18} \\ \text{Diagram 19} \\ \text{Diagram 20} \\ \text{Diagram 21} \\ \text{Diagram 22} \\ \text{Diagram 23} \\ \text{Diagram 24} \\ \text{Diagram 25} \\ \text{Diagram 26} \\ \text{Diagram 27} \\ \text{Diagram 28} \\ \text{Diagram 29} \\ \text{Diagram 30} \\ \text{Diagram 31} \\ \text{Diagram 32} \\ \text{Diagram 33} \\ \text{Diagram 34} \\ \text{Diagram 35} \\ \text{Diagram 36} \\ \text{Diagram 37} \\ \text{Diagram 38} \\ \text{Diagram 39} \\ \text{Diagram 40} \\ \text{Diagram 41} \\ \text{Diagram 42} \\ \text{Diagram 43} \\ \text{Diagram 44} \\ \text{Diagram 45} \\ \text{Diagram 46} \\ \text{Diagram 47} \\ \text{Diagram 48} \\ \text{Diagram 49} \\ \text{Diagram 50} \\ \text{Diagram 51} \\ \text{Diagram 52} \\ \text{Diagram 53} \\ \text{Diagram 54} \\ \text{Diagram 55} \\ \text{Diagram 56} \\ \text{Diagram 57} \\ \text{Diagram 58} \\ \text{Diagram 59} \\ \text{Diagram 60} \\ \text{Diagram 61} \\ \text{Diagram 62} \\ \text{Diagram 63} \\ \text{Diagram 64} \\ \text{Diagram 65} \\ \text{Diagram 66} \\ \text{Diagram 67} \\ \text{Diagram 68} \\ \text{Diagram 69} \\ \text{Diagram 70} \\ \text{Diagram 71} \\ \text{Diagram 72} \\ \text{Diagram 73} \\ \text{Diagram 74} \\ \text{Diagram 75} \\ \text{Diagram 76} \\ \text{Diagram 77} \\ \text{Diagram 78} \\ \text{Diagram 79} \\ \text{Diagram 80} \\ \text{Diagram 81} \\ \text{Diagram 82} \\ \text{Diagram 83} \\ \text{Diagram 84} \\ \text{Diagram 85} \\ \text{Diagram 86} \\ \text{Diagram 87} \\ \text{Diagram 88} \\ \text{Diagram 89} \\ \text{Diagram 90} \\ \text{Diagram 91} \\ \text{Diagram 92} \\ \text{Diagram 93} \\ \text{Diagram 94} \\ \text{Diagram 95} \\ \text{Diagram 96} \\ \text{Diagram 97} \\ \text{Diagram 98} \\ \text{Diagram 99} \\ \text{Diagram 100} \end{array} \right. \quad -0.0112 \alpha^2 R_y, \quad \text{where } R_y = \frac{1}{2} m_\mu \alpha^2$$

Fig. 2.

the usual Lamb shift graphs (muon self energy, anomalous magnetic moment, muon vacuum polarization) give only:

$$\Delta E = 5 \times 10^{-3} \alpha^2 R_y.$$

II. POLARIZABILITY OF THE PROTON AND THE INELASTIC $e-p$ INTERACTIONS

All the above mentioned calculations contain only the static properties of the proton. No effects of the proton dynamics are included. What we are interested in now is the correction to the Lamb shift in ordinary and muonic hydrogen due to the polarizability of the proton in the field of the electron or muon.

In the language of the BSIE it means the inclusion of the kernel (see Fig. 3) which accounts for the dynamical proton structure.

It is easy to see that the result will contain an integration over the inelastic form factors of the proton, obtained from spin independent inelastic electron-proton scattering. We hope that this effect gives only a small correction and the excellent agreement between theory and experiment remains. However, we have no clear evidence that it is really true. As it happened in the problem of the proton-neutron mass difference, some divergence problem could arise. That is also a reason why we are interested in this problem.

$$\Delta J = \left\{ \begin{array}{l} \text{Diagram 1} \\ \text{Diagram 2} \\ \text{Diagram 3} \\ \text{Diagram 4} \\ \text{Diagram 5} \\ \text{Diagram 6} \\ \text{Diagram 7} \\ \text{Diagram 8} \\ \text{Diagram 9} \\ \text{Diagram 10} \\ \text{Diagram 11} \\ \text{Diagram 12} \\ \text{Diagram 13} \\ \text{Diagram 14} \\ \text{Diagram 15} \\ \text{Diagram 16} \\ \text{Diagram 17} \\ \text{Diagram 18} \\ \text{Diagram 19} \\ \text{Diagram 20} \\ \text{Diagram 21} \\ \text{Diagram 22} \\ \text{Diagram 23} \\ \text{Diagram 24} \\ \text{Diagram 25} \\ \text{Diagram 26} \\ \text{Diagram 27} \\ \text{Diagram 28} \\ \text{Diagram 29} \\ \text{Diagram 30} \\ \text{Diagram 31} \\ \text{Diagram 32} \\ \text{Diagram 33} \\ \text{Diagram 34} \\ \text{Diagram 35} \\ \text{Diagram 36} \\ \text{Diagram 37} \\ \text{Diagram 38} \\ \text{Diagram 39} \\ \text{Diagram 40} \\ \text{Diagram 41} \\ \text{Diagram 42} \\ \text{Diagram 43} \\ \text{Diagram 44} \\ \text{Diagram 45} \\ \text{Diagram 46} \\ \text{Diagram 47} \\ \text{Diagram 48} \\ \text{Diagram 49} \\ \text{Diagram 50} \\ \text{Diagram 51} \\ \text{Diagram 52} \\ \text{Diagram 53} \\ \text{Diagram 54} \\ \text{Diagram 55} \\ \text{Diagram 56} \\ \text{Diagram 57} \\ \text{Diagram 58} \\ \text{Diagram 59} \\ \text{Diagram 60} \\ \text{Diagram 61} \\ \text{Diagram 62} \\ \text{Diagram 63} \\ \text{Diagram 64} \\ \text{Diagram 65} \\ \text{Diagram 66} \\ \text{Diagram 67} \\ \text{Diagram 68} \\ \text{Diagram 69} \\ \text{Diagram 70} \\ \text{Diagram 71} \\ \text{Diagram 72} \\ \text{Diagram 73} \\ \text{Diagram 74} \\ \text{Diagram 75} \\ \text{Diagram 76} \\ \text{Diagram 77} \\ \text{Diagram 78} \\ \text{Diagram 79} \\ \text{Diagram 80} \\ \text{Diagram 81} \\ \text{Diagram 82} \\ \text{Diagram 83} \\ \text{Diagram 84} \\ \text{Diagram 85} \\ \text{Diagram 86} \\ \text{Diagram 87} \\ \text{Diagram 88} \\ \text{Diagram 89} \\ \text{Diagram 90} \\ \text{Diagram 91} \\ \text{Diagram 92} \\ \text{Diagram 93} \\ \text{Diagram 94} \\ \text{Diagram 95} \\ \text{Diagram 96} \\ \text{Diagram 97} \\ \text{Diagram 98} \\ \text{Diagram 99} \\ \text{Diagram 100} \end{array} \right\} - \left\{ \begin{array}{l} \text{Diagram 101} \\ \text{Diagram 102} \\ \text{Diagram 103} \\ \text{Diagram 104} \\ \text{Diagram 105} \\ \text{Diagram 106} \\ \text{Diagram 107} \\ \text{Diagram 108} \\ \text{Diagram 109} \\ \text{Diagram 110} \\ \text{Diagram 111} \\ \text{Diagram 112} \\ \text{Diagram 113} \\ \text{Diagram 114} \\ \text{Diagram 115} \\ \text{Diagram 116} \\ \text{Diagram 117} \\ \text{Diagram 118} \\ \text{Diagram 119} \\ \text{Diagram 120} \\ \text{Diagram 121} \\ \text{Diagram 122} \\ \text{Diagram 123} \\ \text{Diagram 124} \\ \text{Diagram 125} \\ \text{Diagram 126} \\ \text{Diagram 127} \\ \text{Diagram 128} \\ \text{Diagram 129} \\ \text{Diagram 130} \\ \text{Diagram 131} \\ \text{Diagram 132} \\ \text{Diagram 133} \\ \text{Diagram 134} \\ \text{Diagram 135} \\ \text{Diagram 136} \\ \text{Diagram 137} \\ \text{Diagram 138} \\ \text{Diagram 139} \\ \text{Diagram 140} \\ \text{Diagram 141} \\ \text{Diagram 142} \\ \text{Diagram 143} \\ \text{Diagram 144} \\ \text{Diagram 145} \\ \text{Diagram 146} \\ \text{Diagram 147} \\ \text{Diagram 148} \\ \text{Diagram 149} \\ \text{Diagram 150} \\ \text{Diagram 151} \\ \text{Diagram 152} \\ \text{Diagram 153} \\ \text{Diagram 154} \\ \text{Diagram 155} \\ \text{Diagram 156} \\ \text{Diagram 157} \\ \text{Diagram 158} \\ \text{Diagram 159} \\ \text{Diagram 160} \\ \text{Diagram 161} \\ \text{Diagram 162} \\ \text{Diagram 163} \\ \text{Diagram 164} \\ \text{Diagram 165} \\ \text{Diagram 166} \\ \text{Diagram 167} \\ \text{Diagram 168} \\ \text{Diagram 169} \\ \text{Diagram 170} \\ \text{Diagram 171} \\ \text{Diagram 172} \\ \text{Diagram 173} \\ \text{Diagram 174} \\ \text{Diagram 175} \\ \text{Diagram 176} \\ \text{Diagram 177} \\ \text{Diagram 178} \\ \text{Diagram 179} \\ \text{Diagram 180} \\ \text{Diagram 181} \\ \text{Diagram 182} \\ \text{Diagram 183} \\ \text{Diagram 184} \\ \text{Diagram 185} \\ \text{Diagram 186} \\ \text{Diagram 187} \\ \text{Diagram 188} \\ \text{Diagram 189} \\ \text{Diagram 190} \\ \text{Diagram 191} \\ \text{Diagram 192} \\ \text{Diagram 193} \\ \text{Diagram 194} \\ \text{Diagram 195} \\ \text{Diagram 196} \\ \text{Diagram 197} \\ \text{Diagram 198} \\ \text{Diagram 199} \\ \text{Diagram 200} \end{array} \right\} + \text{crossed}$$

Fig. 3.

The physical idea behind the polarizability contribution is the following: in a semi-classical picture, the polarizability of the proton means that the instantaneous charge and momentum distribution of the proton can follow the circulating electron. In the limit of a completely polarizable structure, the charge and momentum distribution could completely follow the orbital motion of the electron, and then the proton would appear to it like a point. It is easy to check that within this limit, the finite proton size *plus* the polarizability of the proton result in the decrease of the energy of the atomic level. From this we can conclude immediately that the polarizability contribution always has the effect to decrease the contribution arising from the finite nuclear size, that is, the sign of these corrections will be the opposite one. First let us consider the problem within the non-relativistic model of the proton structure set up by Drell and Sullivan [3].

In this model the proton is composed of a particle (called a quarkette) of the charge $+e$, the mass μ and the spin $1/2$, which satisfies the Schrödinger equation and is bound to a neutral, infinitely massive center-of-force by a non relativistic potential $V(\underline{R})$. The infinite mass center is at the origin, \underline{R} denotes the coordinate of the quarkette and r that of the electron, which is bound to this "physical proton" to form a hydrogen atom. The Hamiltonian for the full system is (see also Fig. 4):

$$H = H_p(\underline{R}) + H_e(\underline{r}) + H_c(\underline{r}, \underline{R}) + H_M(\underline{r}, \underline{R}), \quad (4)$$

$$H_0 \quad \quad \quad H_{int}$$

where: $H_p = P^2/2\mu + V(\underline{R})$, $H_e = (\underline{xp} + \beta m - \alpha/r)$, $H_c = \alpha(1/r - 1/|\underline{r} - \underline{R}|)$, $H_M = \alpha \underline{x} \underline{A}(\underline{r}, \underline{R})$; $\underline{A}(\underline{r}, \underline{R})$ is the vector potential seen by the electron.

In this picture the excited states of the quarkette can be considered as the polarized states of the proton and we can calculate the corresponding contribution to the Lamb shift explicitly.

In the first order perturbation theory only the Coulomb term makes a contribution:

$$v_1^c = \frac{1}{3} \alpha |Y_2(0)|^2 \langle R^2 \rangle_0,$$

where $\langle R^2 \rangle_0$ is the expectation value of the squared radius in the ground state of the quarkette. This is the well-known finite size correction which gives the right numerical value if we fix the quarkette orbit radius in the ground state at the value: $R \sim 2F \sim 10^{-2}$ MeV $^{-1}$. Next we consider the second order perturbation theory. There are three possibilities: 1. the second order in H_c , 2. the second order in H_M , 3. the mixed second order $\sim H_c H_M$.

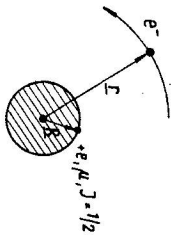


Fig. 4.

I want just briefly to summarize the results as follows:

- there is no contribution from the mixed term;
- there is a small contribution from the second order magnetic interaction which gives:

$$v_2^{MM} \sim \frac{1}{2} \mu_B^2 (m\alpha^3) \left(\frac{m}{M}\right)^3,$$

- the most relevant contribution comes from the second order Coulomb interaction, which gives:

$$v_2^{cc} \sim -(m\alpha^3) \times 10^2 \left(\frac{m}{M}\right)^3.$$

The order of magnitude of this term is:

$$\begin{aligned} &\sim 0.01 \text{ ppm for ordinary-} \\ &\sim 10^{-4} \alpha^2 \text{Ry for muonic-} \end{aligned} \text{-hydrogen.}$$

From this we can conclude that this contribution has a relevant effect in the case of muonic hydrogen, while it is almost negligible in the case of the ordinary hydrogen atom.

It is therefore of some interest to know whether this contribution for muonic hydrogen is measurable or not. The precision of the Lamb-Rutherford experiment for muonic hydrogen is limited because of the instability of the muon.

The order of magnitude of the precision within which the resonance frequencies can be determined is:

$$\hbar\Gamma \sim 5 \times 10^{-4} \alpha^2 \text{Ry}.$$

We can see now that our estimation based on the quarkette model of the proton is comparable with this value.

III. THE RELATIVISTIC TREATMENT OF THE PROBLEM

We shall proceed according to the BSE, and we are interested in the pure polarizability contribution corresponding to the irreducible kernel given in



Fig. 5.

Fig. 5. With the aid of the perturbation theory mentioned above we obtain the contribution to the atomic level shift in the lowest order in α as

$$\Delta E_n = \frac{ie^4}{(2\pi)^3 m_e} |Y_n(0)|^2 \int \frac{d^4q}{q^4} \frac{1}{q^2 - 2m_e v} L_{\mu\nu}(p_e, q) T_{\mu\nu}^S(q^2, \nu), \quad (5)$$

where: $L_{\mu\nu} = g^{\mu\nu}(p_e q) + 2p_e^\mu p_e^\nu$ is the lepton part of the amplitude and $T_{\mu\nu}^S(q^2, \nu)$ is the symmetric or spin-independent part of the virtual forward Compton amplitude, which is defined by

$$T_{\mu\nu} = \frac{i}{4M\pi} \int e^{iqx} \langle P | T(J_\mu(x) J_\nu(0)) | P \rangle.$$

($\nu = (Pq)/M$ is the laboratory photon energy).

With the aid of the invariant expansion

$$T_{\mu\nu}^S(q^2, \nu) = \left(\frac{q_\mu q_\nu}{q^2} - g_{\mu\nu} \right) T_1(q^2, \nu) + \frac{1}{M^2} \left(P_\mu - \frac{M\nu}{q^2} q_\mu \right) \left(P_\nu - \frac{M\nu}{q^2} q_\nu \right) T_2(q^2, \nu)$$

we get

$$\Delta E_n = \frac{ie^4}{(2\pi)^3 m} |Y_n(0)|^2 \int \frac{d^4q}{q^4} \{ T_1(q^2, \nu) F_1(q^2, \nu, m) + T_2(q^2, \nu) F_2(q^2, \nu, m) \},$$

where $F_1(q^2, \nu)$ and $F_2(q^2, \nu)$ are some simple kinematic factors:

$$F_1 = 2m^2 \left(\frac{\nu^2}{q^2} - 1 \right) - 3m\nu$$

$$F_2 = \left(1 - \frac{\nu^2}{q^2} \right) \left[m\nu + 2m^2 \left(1 - \frac{\nu^2}{q^2} \right) \right].$$

In this expression of the level shift the integration variable — the four momentum q_μ — runs over the intergation range so that the variable q^2 may be both positive and negative. Now, the amplitude $T_{\mu\nu}$ for the negative q^2 is measured by combining the electroproduction experiment with the dispersion theory. A simple way to obtain an expression which includes only space-like photons is to make a Wick rotation of the integration contour in the q_0 plane for a fixed q^2 . If we carry out this Cottingham transformation and change the integration variables

$$q_0 \rightarrow iQ_0, \quad \underline{q} \rightarrow \underline{Q},$$

we get

$$\begin{aligned} \Delta E_n = & \frac{e^4}{m(2\pi)^3} |Y_n(0)|^2 \int \frac{d^4Q}{Q^4} \frac{1}{Q^2 + 2miQ_0} \{T_1(-Q^2, iQ_0) + \\ & + T_2(-Q^2, iQ_0) F_2(-Q^2, iQ_0)\}, \end{aligned} \quad (7)$$

where now Q^2 denotes: $Q^2 = Q_0^2 + \underline{Q}^2 = q^2 - q_0^2 = -q^2 \geq 0$, that is $q^2 \leq 0$ and the contribution to the level shift includes only space-like photons.

For the amplitudes T_1 and T_2 we can now write fixed Q^2 dispersion relations in Q_0 . Assuming a Regge behaviour we can write an unsubtracted dispersion relation for T_2 and a one-subtracted dispersion relation for T_1 .

$$\begin{aligned} T_1(q^2, iQ_0) = T_1(q^2, 0) - \frac{Q_0^2}{\pi} \int \frac{d\nu^2 \text{Im} T_1(q^2, \nu)}{\nu^2(q^2 + Q_0^2)} \\ T_2(q^2, iQ_0) = \frac{1}{\pi} \int \frac{d\nu^2 \text{Im} T_2(q^2, \nu)}{\nu^2 + Q_0^2}. \end{aligned}$$

Using next the optical theorem for the Compton scattering

$$\frac{1}{\pi} \text{Im} T_i(q^2, \nu) = \frac{1}{2\pi} W_i(q^2, \nu) \quad i = 1, 2$$

and carrying out the integrations over Q_0 and the angular direction of \underline{Q} , we finally get

$$\begin{aligned} \Delta E_n = & \frac{\alpha^2}{2m_e} |Y_n(0)|^2 \int \frac{dQ^2}{Q^4} \int_{\nu_1}^{\infty} d\nu^2 \{W_1(-Q^2, \nu) F_1(\theta, Q^2, m) + W_2(\dots)_2 \times \\ & \times F_2(\dots)_1\}, \end{aligned} \quad (8)$$

where F_1 and F_2 are now kinematic factors, complicated functions of $\nu = \nu^2/Q^2$, Q^2 and the lepton mass m .

To get the final numerical result we have to carry out the integration in the physical region of the entire $q^2 - \nu$ plane. This requires the knowledge of the electron-proton inelastic scattering data in the entire kinematic region ($q^2 \leq 0$, $\omega \geq 1$). For this purpose one can use the Breidenbach-Kuti fit [6] of the inelastic electron-proton scattering data based on the SLAC-MIT measurements.

With the aid of this fit we can calculate the numerical value of the level shift. We find that the most relevant contribution comes from the exchange of low energy photons of small or zero mass ($q^2 \ll M_p^2$, $\nu \lesssim 1$ GeV). It is therefore not surprising that the result can be expressed in terms of the dynamical electric and magnetic polarizabilities of the proton (α_{p0l} and β_{p0l}), for which the following sum rule holds:

$$\alpha_{p0l} + \beta_{p0e} = \frac{1}{4\pi^2} \int_{\nu_1}^{\infty} \frac{d\nu}{\nu^2} \sigma_T(\nu), \quad (9)$$

where $\sigma_T(\nu)$ is the total cross section of the Compton scattering for real photons as a function of the laboratory photon energy. This nice relation can be obtained by using low energy theorems and dispersion relations.

A numerical estimation for α_{p0l} and β_{p0l} using photoproduction data up to $\nu = 1$ GeV gives the result

$$\alpha_{p0l} + \beta_{p0l} = 1.0 \times 10^{-42} \text{ cm}^2 \sim \frac{1}{8M_p^3}$$

The final result in terms of the dynamic polarizabilities of the proton is

$$\Delta E_n \cong -2m_e \alpha |Y_n(0)|^2 (\alpha_{p0l} + \beta_{p0l}) \left(\ln \frac{M_p}{m_e} + 2 \right), \quad (10)$$

which gives the numerical value

$$\Delta E_n \sim 54 \text{ Hz} \sim 0.05 \text{ ppm}$$

for the hydrogen atom, which is almost negligible compared to the precision of the measurement (~ 50 ppm).

No divergence problem arises. This can be connected with the fact that because of the two photon and one electron propagator $\Delta E_n \sim \int \frac{d^4k}{k^6}$, while the neutron-proton mass difference $\Delta M \sim \int k^{-2} d^4k$, which is divergent for large k . In the case of muonic hydrogen we get the result simply using the muon-electron universality

$$\Delta E_n \simeq -2m_\mu \alpha |\Psi_n(0)|^2 (\alpha_{\text{prol}} + \beta_{\text{prol}}) \left(\ln \frac{M_p}{m_\mu} + 2 \right) = 4.121 \times \\ \times 10^3 \text{ MHz} \sim 80 \text{ ppm}$$

which is comparable with the precision of the measurement (100 ppm).

IV. COMMENTS AND CONCLUSIONS

Finally I should like to mention an argument why the calculation of this contribution to the Lamb shift of muonic hydrogen can be important. This argument is connected with the possible existence of some muon-electron differences. If we assume that the muon is not simply a „fat electron“, the difference between these two particles is not only a difference in mass and associated neutrinos, but there are other differences for example the muon has a special interaction with hadrons — we can search for effects of these differences. If there existed such a special muon-hadron interaction, it would have the effect to produce anomalies in the spectra of muonic hydrogen.

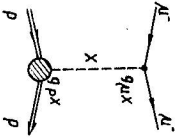


Fig. 6.

Assuming that the muon interacts with hadrons through the exchange of a neutral hadron X (mass M_X , coupling to the muon $g_{\mu X}$ to hadrons $g_{p X}$) the contribution of this effect to the Lamb shift compared to the contribution arising from the two-photon exchange process is (see also Fig. 6):

$$\delta_X = \frac{E_X}{E_2} = \frac{16\pi g_{\mu X} g_{p X} M_p M_p^2}{5 e^2 m_\mu M_X^2} \quad (11)$$

Present experimental data [5] on the parameters M_X , $g_{\mu X}$ and $g_{p X}$ allow:

$$\frac{g_{\mu X} g_{p X}}{e^2} \lesssim 0.05 \quad \text{and} \quad M_X^2 = (0.2 \pm 0.4) M_p^2.$$

Thus we can conclude that using these limits the δ_X ration can exceed the value 10—50 and in this case this process would have a well measurable effect on the spectra of muonic hydrogen.

Well, this is a reason why the exact calculation of the two-photon exchange contribution is important. We have seen that this effect gives only a correction just comparable with the precision of the measurement. Furthermore it is well known that other higher order electromagnetic processes give only undetectable effects. Thus if future measurements showed a significant anomaly in the spectra of muonic hydrogen, it would suggest the existence of such an anomalous muon-hadron interaction. On the other hand: if the measurements does not give such a significant anomaly, we can — on the basis of the estimation (11) — get stronger restrictions on the parameters (M_X , $g_{\mu X}$, $g_{p X}$) of the anomalous muon-hadron interaction.

REFERENCES

- [1] Salpeter E. E., Phys. Rev. *87* (1952), 328.
- [2] Di Giacomo A., CERN-TH.1006 (1969).
- [3] Drell S., Sullivan D., Phys. Rev. *154* (1967), 1477.
- [4] Choudhury S. R., Freedman D. Z., Phys. Rev. *168* (1968), 1739.
- [5] Perl M. et al., SLAC-PUB-1009 (1972).
- [6] Breidenbach M., Kuti J., Physics Letters *41 B* (1972), 345.

Received April 19th, 1973